International Journal of Research
Available at https://edupediapublications.org/journals
e-ISSN: 2348-6848
p-ISSN: 2348-795X
Volume 04 Issue 13
October 2017

Multilevel -Based Cascaded Two-Level Solar PV Inverter STATCOM for High-Power Applications

Bandi Sumalatha[1], Ralla Ramya [2], Bomma Shwetha[3]

[1] M.Tech POWER ELECTRONICS in 2017 JNTUH, Hyderabad, Telangana, India.
bandisumalatha3@gmail.com
[2] M.Tech POWER ELECTRONICS AND ELECTRIC DRIVES JNTUH, Telangana ,India.
sharanya.ramya46@gmail.com
[3] M.Tech POWER ELECTRONICS JNTUH *Hyderabad, Telangana, India.*
bommaswethapatel@gmail.com

Abstract— *In this paper, a simple static var compensating scheme using a cascaded two-level inverter-based multilevel inverter is proposed. The topology consists of two standard two-level inverters connected in cascade through open-end windings of a three-phase transformer. The dc-link voltages of the inverters are regulated at different levels to obtain four-level operation. The simulation study is carried out in MATLAB/SIMULINK to predict the performance of the proposed scheme under balanced and unbalanced supply-voltage conditions. A laboratory prototype is developed to validate the simulation results. The control scheme is implemented using the Further, stability behavior of the topology is investigated. The dynamic model is developed and transfer functions are derived. The system behavior is analyzed for various operating conditions.*

Index Terms—DC-link voltage balance, multilevel inverter, power quality (PQ), staticcompensator(STATCOM).

I. INTRODUCTION

The application of flexible ac transmission systems (FACTS) controllers, such as static compensator (STATCOM) and static synchronous series compensator (SSSC), is increasing in power systems. This is due to their ability to stabilize the transmission systems and to improve power quality (PQ) in distribution systems. STATCOM is popularly accepted as a reliable reactive power controller replacing conventional var compensators, such as the thyristor-switched capacitor (TSC) and thyristor-controlled reactor (TCR). This device provides reactive power compensation, active power oscillation damping, flicker attenuation, voltage regulation, etc. Generally, in high-power applications, var compensation is achieved using multilevel inverters [2]. These inverters consist of a large number of dc sources which are usually realized by capacitors. Hence, the converters draw a small amount of active power to maintain dc voltage of capacitors and to compensate the losses in the converter. However, due to mismatch in conduction and switching losses of the switching devices, the capacitors voltages are unbalanced. Balancing these voltages is a major research challenge in multilevel inverters. Various control schemes using different topologies are reported. Among the three conventional multilevel inverter topologies, cascade H-bridge is the most popular for static var compensation [5], [6]. A multilevel converter not only achieves high power ratings, but also enables the use of renewable energy sources. Renewable energy sources such as photovoltaic, wind, and fuel cells can be easily interfaced to a multilevel converter system for a high power application [1-3]. The concept of multilevel converters has been introduced since 1975 [4]. The term multilevel began with the three-level converter [5]. Subsequently, several multilevel converter topologies have been developed [6-13]. However, the elementary concept of a multilevel converter to achieve higher power is to use a series of power semiconductor switches with several lower voltage dc sources to perform the power conversion by synthesizing a staircase voltage waveform. Capacitors, batteries, and renewable energy voltage sources can be used as the multiple dc voltage sources. The commutation of the power switches

International Journal of Research
Available at https://edupediapublications.org/journals
e-ISSN: 2348-6848
p-ISSN: 2348-795X
Volume 04 Issue 13
October 2017

aggregate these multiple dc sources in order to achieve high voltage at the output; however, the rated voltage of the power semiconductor switches depends only upon the rating of the dc voltage sources to which they are connected. A multilevel converter has several advantages over a conventional two-level converter that uses high switching frequency pulse width modulation (PWM). The attractive features of a multilevel converter can be briefly summarized as follows. ● Staircase waveform quality: Multilevel converters not only can generate the output voltages with very low distortion, but also can reduce the dv/dt stresses; therefore electromagnetic compatibility (EMC) problems can be reduced. ● Common-mode (CM) voltage: Multilevel converters produce smaller CM voltage; therefore, the stress in the bearings of a motor connected to a multilevel motor drive can be reduced. Furthermore, CM voltage can be eliminated by using advanced modulation strategies such as that proposed in [14]. ● Input current: Multilevel converters can draw input current with low distortion. ● Switching frequency: Multilevel converters can operate at both fundamental switching frequency and high switching frequency PWM. It should be noted that lower switching frequency usually means lower switching loss and higher efficiency. Unfortunately, multilevel converters do have some disadvantages. One particular disadvantage is the greater number of power semiconductor switches needed. Although lower voltage rated switches can be utilized in a multilevel converter, each switch requires a related gate drive circuit. This may cause the overall system to be more expensive and complex.

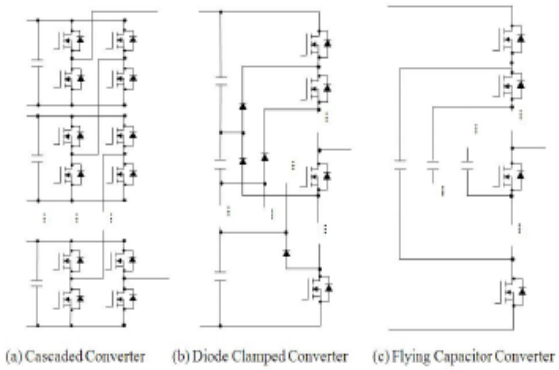

Fig.1 Typical Circuit Topologies of Multilevel Inverters.

In this paper, a static var compensation scheme is proposed for a cascaded two-level inverter-based multilevel inverter. The topology uses standard two-level inverters to achieve multilevel operation. The dc-link voltages of the inverters are regulated at asymmetrical levels to obtain four-level operation. To verify the efficacy of the proposed control strategy, the simulation study is carried out for balanced and unbalanced supply-voltage conditions. A laboratory prototype is also developed to validate the simulation results. From the detailed simulation and experimentation by the authors, it is found that the dc-link voltages of two inverters collapse for certain operating conditions when there is a sudden change inreference current. In order to investigate the behavior of the converter, the complete dynamic model of the system is developed from the equivalent circuit. The model is linearized and transfer functions are derived. Using the transfer functions, system behavior is analyzed for different operating conditions. This paper is organized as follows: The proposed control scheme is presented in Section II. Stability analysis of the converter is discussed in Section III. Simulation and experimental results are presented in Sections IV and V, respectively

II. MODELING OF PROPOSED THEORYCASCADED TWO-LEVEL INVERTER-BASED MULTI LEVEL STATCOM:

Fig. 1 shows the power system model Fig. 2 shows the circuit inverter-based multilevel STATCOM using standard two-level inverters. The inverters are connected on the low-voltage (LV)side of the transformer and the high-voltage (HV) side is connected to the grid. The dc-link voltages of the inverters are maintained constant and modulation indices are controlled to achieve the required objective. The proposed control scheme is derived from the ac side of the equivalent circuit which is shown in Fig. 3. In the figure, $v_a^{'}, v_b^{'}$ and $v_c^{'}$ are the source voltages referred to LV side of the transformer,r_a, r_b and r_c are the resistances which represent the losses in the transformer and two inverters,L_a, L_b and L_c are leakage inductances of

International Journal of Research
Available at https://edupediapublications.org/journals
e-ISSN: 2348-6848
p-ISSN: 2348-795X
Volume 04 Issue 13
October 2017

transformer windings, and e_{a1}, e_{b1}, e_{c1} and e_{a2}, e_{b2}, e_{c2} are the output voltages of inverters 1 and 2, respectively. r_1, r_2 are the leakage resistances of dc-link capacitors c_1 and c_2, respectively. Assuming $r_a = r_b = r_c = r$, $L_a = L_b = L_c = L$ and applying KVL on the ac side, the dynamic model can be derived using[14] as topology of the cascaded two-level

$$\begin{bmatrix} \frac{di_a}{dt} \\ \frac{di_b}{dt} \\ \frac{di_c}{dt} \end{bmatrix} = \begin{bmatrix} \frac{1}{L} & 0 & 0 \\ 0 & \frac{-r}{L} & 0 \\ 0 & 0 & \frac{-r}{L} \end{bmatrix} \begin{bmatrix} i_a \\ i_b \\ i_c \end{bmatrix} + \frac{1}{L} \begin{bmatrix} v_a - (e_{a1} - e_{a2}) \\ v_b - (e_{b1} - e_{b2}) \\ v_c - (e_{c1} - e_{c2}) \end{bmatrix} \quad (1)$$

Equation (1) represents the mathematical model of the cascaded two-level inverter-based multilevel STATCOM in the stationary reference frame. This model is transformed to the synchronously rotating reference frame [14]. The – axes reference voltage components of the converter and are controlled as

$$e_d^* = x_1 - \omega L i_q + v_d \quad (2)$$

$$e_q^* = x_2 + \omega L i_d + v_q \quad (3)$$

where v_d is the d-axis voltage component of the ac source and i_d, i_q are d-q axes current components of the cascaded inverter, respectively. The synchronously rotating frame is aligned with source voltage vector so that the q-component of the source voltage v_d is made zero. The control parameters and are controlled as follows:

$$x_1 = \left(k_{p1} + \frac{k_{i1}}{s}\right)(i_d^* - i_d) \quad (4)$$

$$x_2 = \left(k_{p2} + \frac{k_{i2}}{s}\right)(i_q^* - i_q). \quad (5)$$

The d-axis reference current i_d, is obtained as

$$i_d^* = \left(k_{p3} + \frac{k_{i3}}{s}\right)\left[(V_{dc1}^* + V_{dc2}^*) - (V_{dc1} + V_{dc2})\right] \quad (6)$$

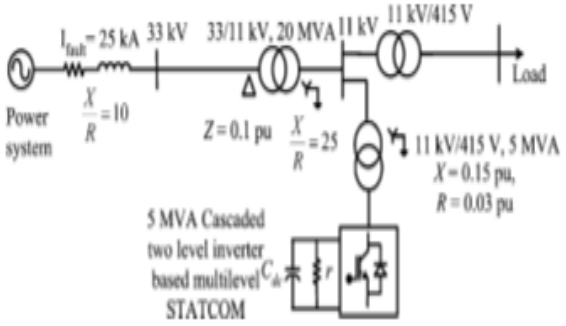

Fig. 1. Power system and the STATCOM model.

Three-phase grid-connected PV system

The schematic diagram of a three-phase grid-connected PV system, which is the main focus of this thesis, is shown in Fig. 3.3. The considered PV system consists of

1. A PV array
2. A dc-link capacitor *C*
3. A three-phase inverter
4. A filter inductor *L*
5. Grid voltages

The objective of this thesis is to control the voltage Vdc(which is also the output voltage of PV array) across the capacitor *C*.

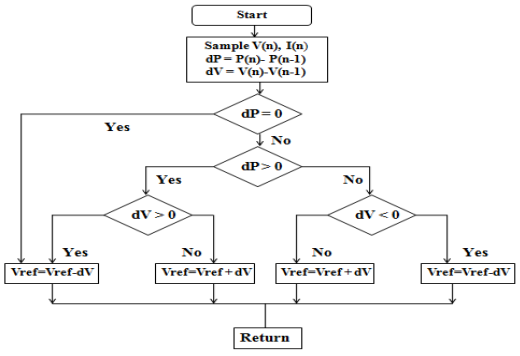

Fig.3.5 Flow chart of perturb and observe

3.6 Uncertainties in PV system

International Journal of Research
Available at https://edupediapublications.org/journals
e-ISSN: 2348-6848
p-ISSN: 2348-795X
Volume 04 Issue 13
October 2017

In a practical PV system, atmospheric conditions change continuously for which there exists a variation in cell working temperature, as well as in solar irradiance. Because of changes in atmospheric conditions, the output voltage, current, and power of the PV unit changes significantly. For example, if a single module of a series string is partially shaded, and then its output current will be reduced, which will change the operating point of the whole string.

Since the amount of the PV generation depends on solar irradiation that is uncertain, there are uncertainties in output current of PV array which in turn causes uncertainties in the current injected into the grid. Moreover, as the values of the parameters used in the PV model are not exactly known, there are also parametric uncertainties. The PV system model cannot capture these uncertainties. Therefore, it is essential to consider these uncertainties within the PV system model.

3.7 Various uncertainties in PV system

1. Variations in solar irradiation
2. Variation in solar cell temperature
3. Partial shading scenario
4. Snow fall
5. Dirt and Soiling
6. Power rating of modules
7. Degradation or Ageing of PV modules
8. Parametric uncertainties

3.7.1 Variations in solar irradiation

Usually under the standard atmospheric conditions, the solar irradiation is 1000 W/sq.m. The I-Vcharacteristic of the PV module for different irradiances but under the constant temperature of $25^{o}C$ are shown in Fig. 3.4.

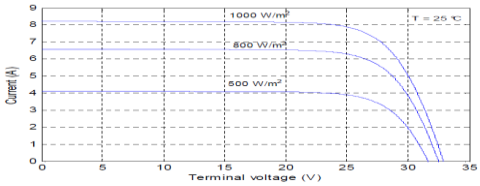

Fig.3.6 I-V characteristics of the PV module under different solar irradiation levels

From Fig.3.4, it is observed that, as the solar irradiation increases, the output current increases and the output voltage slightly increases. The P-Vcharacteristic of the PV module for different irradiances under the constant temperature of $25^{o}C$ are shown in Fig.3.5.

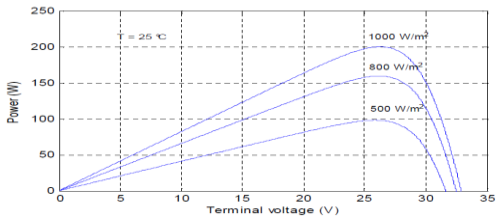

Fig3.7 P-V characteristics of the PV module under different solar irradiation levels

3.4.2 Variation in solar cell temperature

Like all other semiconductor devices, solar cells are sensitive to temperature. Increasing the temperature reduces the band gap of a semiconductor, thereby effecting most of the semiconductor material parameters. The decrease in the band gap of a semiconductor with increasing temperature can be viewed as increasing the energy of the electrons in the material. Lower energy is therefore needed to break the bond. In the bond model of a semiconductor band gap, reduction in the bond energy also reduces the band gap. Therefore increasing the temperature reduces the band gap.

A PV module will be typically rated at 25 °C under 1 kW/m^2. However, when operating in the field, they typically operate at higher temperatures and at somewhat lower insolation conditions. In order to determine the power output of the solar cell, it is important to determine the expected operating temperature of the PV module. The nominal operating cell temperature is defined as the temperature reached by open circuited cells in a module under the conditions as listed below:

1. Irradiance on cell surface = 800 W/m^2
2. Air temperature = 20°C
3. Wind velocity = 1 m/s
4. Mounting = open back side

In a solar cell, the parameter most affected by an increase in temperature is the open-circuit voltage. Usually under the standard atmospheric conditions, the solar cell temperature is $25^{o}C$. The

International Journal of Research
Available at https://edupediapublications.org/journals
e-ISSN: 2348-6848
p-ISSN: 2348-795X
Volume 04 Issue 13
October 2017

I-Characteristics of the PV module for different temperatures but under the constant solar irradiation of 1000 W/sq.m are shown in Fig. 3.6. It can also be observed that the variations of the irradiance slightly changes with open-circuit voltage.

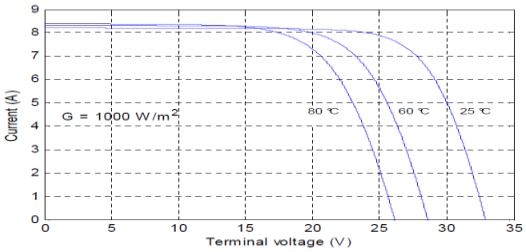

Fig.3.8 I-V characteristics of the PV module at different surface temperatures

From Fig.3.6, it is observed that, as the PV module temperature increases, the output current is slightly increases and the output voltage increases. The P-Vcharacteristic of the PV module for different temperatures and with the constant solar irradiation of 1000 W/sq.m are shown in Fig.3.7.

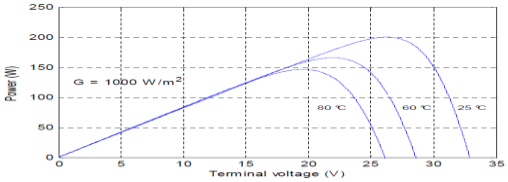

Fig.3.9 P-V characteristics of the PV module at different surface temperatures

3.4.3 Partial shading scenario

Shading may occur due to clouds, environmental obstructions such as trees and buildings, self-shading between panels in parallel rows, dirt and dust, bird droppings etc. These shading effects may be static, i.e. slow due to sunlight angle during the day or may be very dynamic (e.g. moving

Partial shading can be minimized by using bypass and blocking diodes as shown in Fig.3.11

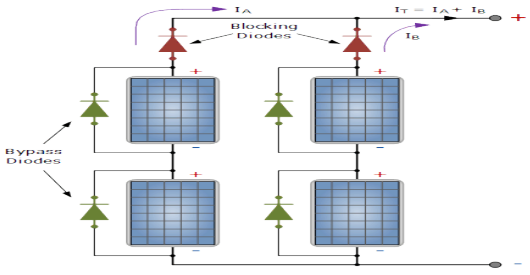

Fig.3.11 Bypass and blocking diodes

Bypass diode is connected in parallel to the PV cell to bypass the shaded cell and avoid hotspot. Blocking diode blocks circulating current flow through the parallel connected PV strings.

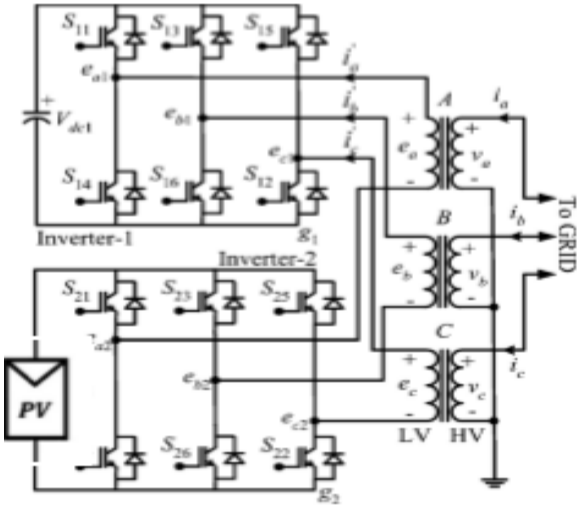

Fig. 2. Cascaded two-level inverter-based multilevelSTATCOM.

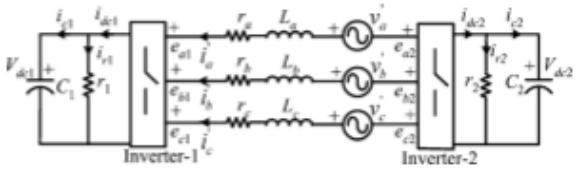

Fig. 3. Equivalent circuit of the cascaded two-level inverter-based multilevel STATCOM.

A. Control Strategy

The control block diagram is shown in Fig. 4. The unit signals and are generated from the phase-locked loop (PLL) using three-phase supply voltages [14]. The converter currents are transformed to the synchronous rotating reference frame using the unit signals. The switching frequency ripple in the converter current components is eliminated using a low-passfilter (LPF). From and loops, the controller generates – axes reference voltages, and for the cascaded inverter. With these reference voltages, the

International Journal of Research
Available at https://edupediapublications.org/journals
e-ISSN: 2348-6848
p-ISSN: 2348-795X
Volume 04 Issue 13
October 2017

inverter supplies the desired reactive current and draws required active current to regulate total dc-link voltage . However, this will not ensure that individual dc-link voltages are controlled at their respective reference values. Hence, additional control is required to regulate individual dc-link voltages of the inverters.

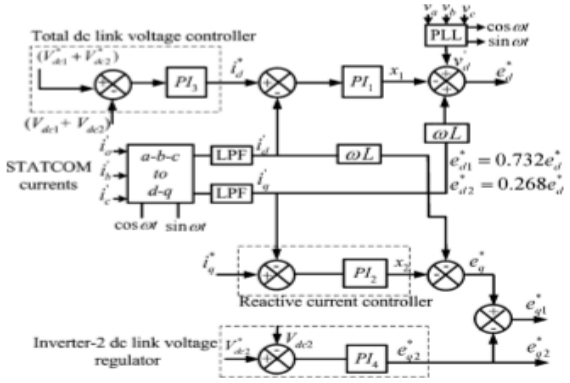

Fig. 4. Control block diagram.

B. DC-Link Balance Controller

The resulting voltage of the cascaded converter can be given As $e_I \angle \delta$, where $e_I = \sqrt{e_d^2 + e_q^2}$ and $\delta = \tan^{-1}((e_q)/(e_d))$. The active power transfer between the source and inverter depends on and is usually small in the inverters supplying var to the grid [1]. Hence, can be assumed to be proportional to e_q. Therefore, the -axis reference voltage component of inverter-2

is derived to control the dc-link voltage of inverter-2 ast he q-axis reference voltage component of inverter-1 is obtained as

The dc-link voltage of inverter-2 v_{dc2} is controlled at 0.366 times the dc-link voltage of inverter-1 v_{dc1}. It results in four-level operation in the output voltage and improves the harmonic spectrum. Expressing dc-link voltages of inverter-1 and inverter-2 in terms of total dc-link voltage, v_{dc} as

$$V_{dc1} = 0.732 V_{dc} \quad (9)$$

$$V_{dc2} = 0.268 V_{dc}. \quad (10)$$

Since the dc-link voltages of the two inverters are regulated, the reference d-axis voltage component v_d^* is divided in between the two inverters in proportion to their respective dc-link voltage as

$$e_{d1}^* = 0.732 e_d^* \quad (11)$$

$$e_{d2}^* = 0.268 e_d^*. \quad (12)$$

C. Unbalanced Conditions

Network voltages are unbalanced due to asymmetric faults or unbalanced loads [16]. As a result, negative-sequence voltage appears in the supply voltage. This causes a double supply frequency component in the dc-link voltage of the inverter. This double frequency component injects the third harmonic component in the ac side [17]. Moreover, due to negative-sequence voltage, large negative-sequence current flows through the inverter which may cause the STATCOM to trip [16]. Therefore, during unbalance, the inverter voltages are controlled in such a way that either negative-sequence current flowing into the inverter is eliminated or reduces the unbalance in the grid voltage. In the latter case, STATCOM needs to supply large currents since the interfacing impedance is small. This may lead to tripping of the converter.

The negative-sequence reference voltage components of the inverter e_{dn}^* and e_{qn}^* are controlled similar to positive-sequence components in the negative synchronous rotating frame as

$$e_{dn}^* = -x_3 + (-\omega L_s) i_{qn}' - v_{dn}' \quad (13)$$

$$e_{qn}^* = -x_4 - (-\omega L_s) i_{dn}' + v_{qn}' \quad (14)$$

The control parameters x_3 and x_4 are controlled as follows:

$$x_3 = \left(k_{p3} + \frac{k_{i3}}{s}\right)\left(i_{dn}^* - i_{dn}'\right) \quad (15)$$

$$x_4 = \left(k_{p4} + \frac{k_{i4}}{s}\right)\left(i_{qn}^* - i_{qn}'\right). \quad (16)$$

The reference values for negative-sequence current components i_{dn}^* and i_{qn}^* are set at zero to block negative-sequence current from flowing through the inverter.The system may exhibit oscillatory

International Journal of Research
Available at https://edupediapublications.org/journals
e-ISSN: 2348-6848
p-ISSN: 2348-795X
Volume 04 Issue 13
October 2017

instability when there is a step change in reference for highcontroller gains. Therefore, the controller gains should be designed suitably to avoid the instability. This behavior is similar to that of the two-level inverter-based STATCOM.

III. SIMULATION RESULTS

The system configuration shown in Fig. 1 is considered for simulation. The simulation study is carried out using MATLAB/SIMULINK. The system parameters are given in Table I.

TABLE I
SIMULATION SYSTEM PARAMETERS

Rated power	5 MVA
Transformer voltage rating	11kV/400
AC supply frequency, f	50 Hz
Inverter-1 dc link voltage, V_{dc1}	659 V
Inverter-2 dc link voltage, V_{dc2}	241 V
Transformer leakage reactance, X_l	15%
Transformer resistance, R	3%
DC link capacitances, C_1, C_2	50 mF
Switching frequency	1200 Hz

A. Reactive Power Control

In this case, reactive power is directly injected into the grid by setting the reference reactive current component at a particular value. Initially i_q^*, issetat0.5p.u.At t=2.0 s, i_q^*, is changed to -0.5 p.u. Fig. 7(a) shows the source voltage and converter current of the A-phase. Fig. 7(b) shows the dc-link voltages of two inverters. From thefigure, it can be seen that the dc-link voltages of the inverters are regulated at their respective reference values when the STATCOM mode is changed from capacitive to inductive. Moreover, the dc-link voltage of inverter2 attains its reference value faster compared to that of inverter1 as discussed in Section II.

B. Load Compensation

In this case, the STATCOM compensates the reactive power of the load. Initially, STATCOM is supplying a current of 0.5 p.u. At t=2.0 s, the load current is increased so that STATCOM supplies its rated current of 1 p.u. Fig. 8(a) shows source voltage and converter current, while Fig. 8(b) shows the dc-link voltages of two inverters. The dc-link voltages are maintained at their respective reference values when the operating conditions are changed.

C. Operation During the Fault Condition

In this case, a single-phase-to-ground fault is created at t=1.2s,on the A-phase of the HV side of the 33/11-kV transformer. The fault is cleared after 200 ms. Fig. 9(a) shows voltages across the LV side of the 33/11-kV transformer. Fig. 9(b) and (c) shows the d-q axes components of negative-sequence current of the converter. These currents are regulated at zero during the fault condition.

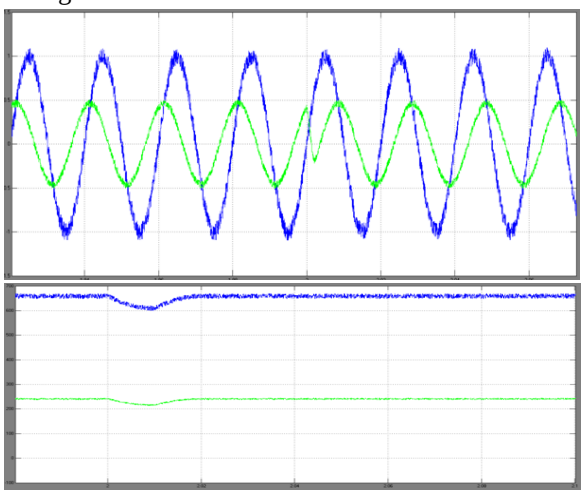

Fig. 7. Reactive power control. (a) Source voltage and inverter current. (b) DC-link voltages of two inverters

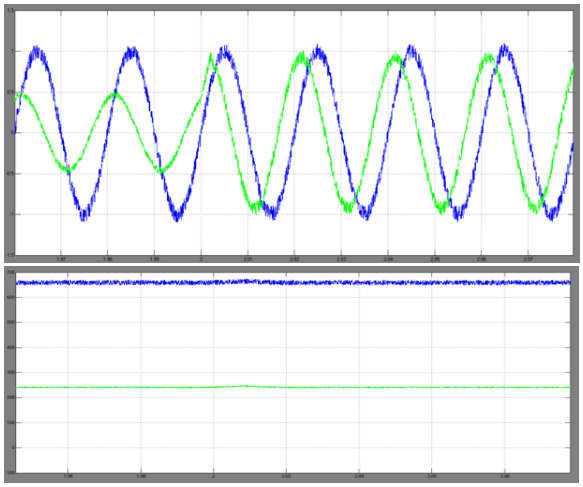

Fig. 8. Load compensation. (a) Source voltage and inverter current. (b) DC-link voltages of two inverters.

b) With Negative-Sequence Controller: In this case, the negative-sequence controllerrepresented by (13) and (14) is enabled along with the positive-sequence controller. The references for inverter negative-sequence current components $i^*_{dn}$and i^*_{qn} are set at zero. Therefore, the inverter supplies balanced currents as shown in Fig. 13(a). Fig. 13(b) shows the dc-link voltages of two inverters. The oscillations in the dc-link voltages of two inverters are reduced compared to those in Fig. 12(b).

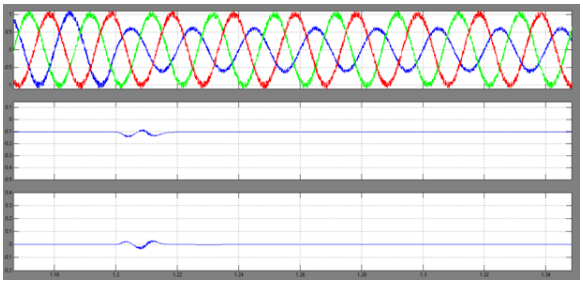

Fig. 9. Operation during fault. (a) Grid voltages on the LV side of the transformer. (b) -axis negative-sequence current component . (c) -axis negative-sequence current component .

IV. CONCLUSION

DC-link voltage balance is one of the major issues in cascaded inverter-based STATCOMs. In this paper, a simple var compensating scheme is proposed for a cascaded two-level inverter-based multilevel inverter. The scheme ensures regulation of dc-link voltages of inverters at asymmetrical levels and reactive power compensation. The performance of the scheme is validated by simulation and experimentations under balanced and unbalanced voltage conditions. Further, the cause for instability when there is a change in reference current is investigated. The dynamic model is developed and transfer functions are derived. System behavior is analyzed for various operating conditions. From the analysis, it is inferred that the system is a nonminimum phase type, that is, poles of the transfer function always lie on the left half of the s-plane. However, zeros shift to the righthalfofthe s-plane for certain operating conditions. For such a system, oscillatory instability for high controller gains exists.

V. REFERENCES

[1] N. G. Hingorani and L. Gyugyi, Understanding FACTS. Delhi, India: IEEE, 2001, Standard publishers distributors.

[2] B. Singh, R. Saha, A. Chandra, andK. Al-Haddad, "Static synchronous compensators (STATCOM): A review,"IET Power Electron., vol. 2, no. 4, pp. 297–324, 2009.

[3] H. Akagi, H. Fujita, S. Yonetani, and Y. Kondo, "A 6.6-kV transformerless STATCOM based on afive-level diode-clamped PWM converter: System design and experimentation of a 200-V 10-kVA laboratory model," IEEE Trans. Ind. Appl., vol. 44, no. 2, pp. 672–680, Mar./Apr. 2008.

[4] A. Shukla, A. Ghosh, and A. Joshi, "Hysteresis current control operation offlying capacitor multilevel inverter and its application in shunt compensation of distribution systems,"IEEE Trans. Power Del., vol. 22, no. 1, pp. 396–405, Jan. 2007.

[5] H. Akagi, S. Inoue, and T. Yoshii, "Control and performance of a transformerless cascaded PWM STATCOM with star configuration,"IEEE Trans. Ind. Appl., vol. 43, no. 4, pp. 1041–1049, Jul./Aug. 2007.

[6] Y. Liu, A. Q. Huang, W. Song, S. Bhattacharya, and G. Tan, "Smallsignal model-based control strategy for balancing individual dc capacitor voltages in cascade multilevel inverter based STATCOM," IEEE Trans. Ind. Electron., vol. 56, no. 6, pp. 2259–2269, Jun. 2009.

[7] H.P.MohammadiandM.T.Bina,"Atransformerless medium-voltage STATCOM topology based on extended modular multilevel converters,"IEEE Trans. Power Electron., vol. 26, no. 5, pp. 1534–1545, May 2011.

[8] X. Kou, K. A. Corzine, and M. W. Wielebski, "Overdistention operation of cascaded multilevel inverters,"IEEE Trans. Ind. Appl., vol. 42, no. 3, pp. 817–824, May/Jun. 2006.

[9] K. K. Mohaptra, K. Gopakumar, and V. T. Somasekhar, "A harmonic elimination and suppression scheme for an open-end winding induction motor drive,"IEEE Trans. Ind. Electron., vol. 50, no. 6, pp. 1187–1198, Dec. 2003.

[10] Y. Kawabata, N. Yahata, M. Horii, E. Egiogu, and T. Kawabata, "SVG using open winding transformer and two inverters," inProc., 35th Annual IEEE Power Electron. Specialists Conf., 2004, pp. 3039–3044.

[12] N. N. V. Surendra Babu, D. Apparao, and B. G. Fernandes, "Asymmetrical dc link voltage balance of a cascaded two level inverter based STATCOM," inProc., IEEE TENCON, 2010, pp. 483–488.

[13] IEEE Criteria for Class IE Electric Systems, IEEE Standard 141-1993.

BANDI SUMALATHA

Completed B.Tech in Electrical & Electronics Engineering in 2013 under JNTU UNIVERSITY, HYDERABAD andM.TechPOWERELECTRONICS in 2017 under JNTUH,Hyderabad,Telangana,India.
Email id: **bandisumalatha3@gmail.com**

RALLA RAMYA

Completed B.Tech in Electrical & Electronics Engineering in 2015 under JNTUH and M.Tech (POWER ELECTRONICS AND ELECTRIC DRIVES) under JNTUH, Telangana ,India. Area of nterest include Power systems and Power Electronics.
Email id: **sharanya.ramya46@gmail.com**

.

BOMMA SHWETHA

Completed B.Tech in Electrical & Electronics Engineering in 2014 under JNTU UNIVERSITY,HYDERABAD and M.Tech(POWER ELECTRONICS) in 2016 under JNTUH, Hyderabad, Telangana, India. I am working as an assistant professor. Area of interest includes power electronics.
E-mail id**;** **bommaswethapatel@gmail.com**